Carbohydrate Polymers 104 (2014) 50–58

Contents lists available at ScienceDirect

Carbohydrate Polymers

journal homepage: www.elsevier.com/locate/carbpol

Characterization of a new biodegradable edible film made from salep glucomannan

Abdullah Kurt [a,c], Talip Kahyaoglu [a,b,*]

[a] Department of Food Engineering, Engineering Faculty, Ondokuz Mayıs University, 55139, Samsun, Turkey
[b] Department of Food Engineering, Chemistry-Metallurgical Faculty, Yıldız Technical University, 34210 Istanbul, Turkey
[c] Department of Food Engineering, Engineering and Architecture Faculty, Bitlis Eren University, 13000 Bitlis, Turkey

ARTICLE INFO

Article history:
Received 1 November 2013
Received in revised form
16 December 2013
Accepted 2 January 2014
Available online 9 January 2014

Keywords:
Edible films
Salep
Glucomannan
Galactomannan
Film properties
Rheology

ABSTRACT

The aims of this study were to report the film-forming properties of salep glucomannan (SG) and characterize its physical, barrier, mechanical, sorption and thermal properties for the first time. Galactomannan films (LBG, locust bean gum; GG, guar gum) were also prepared to compare with SG films. The steady and oscillatory rheological behaviors of the film solution were evaluated. The viscosity of the SG was less dependent than that of LBG and GG on temperature. The physical properties of SG films showed good potential for food applications. The oxygen and water vapor barrier properties of SG were better than LBG and GG films. SG film was less mechanically resistant than LBG but more flexible than galactomannan films. The highest transition temperature (T_g) was determined to be $-11.46 \pm 0.65\,^{\circ}C$ for SG film. The results showed that SG has good potential for use in producing an edible film for various food applications.

1. Introduction

Mannans are one of the most abundant hemicelluloses present as supporting and storage polysaccharides in the cell wall, legume seeds, and plant tubers (Mikkonen, 2009; Rowell, Pettersen, Han, Rowell, & Tshabalala, 2005). The gums from leguminous seeds (locust bean gum, LBG; guar gum, GG) and plant tubers (konjac glucomannan, KGM, from *Amorphophallus konjac*; salep glucomannan, SG, from the *Orchidaceae* family) are classified as mannans. Glucomannan is a chain consisting of glucose and mannose connected by β-(1→4) glycosidic bonds. Galactomannan is linked by β-(1→4) glycosidic bonds, with a galactose substitution at the C-6 position. These high molecular weight polymers are known as hydrocolloids and interact strongly with water. Hydrocolloids are used in the food industry for their thickening, gelling, stabilizing, texture-modification and film-forming properties. Salep has also received considerable attention for the same purposes (Farhoosh & Riazi, 2007; Pourjavadi, Fakoorpoor, & Hosseine, 2013).

Salep is the roots or tubers of *Orchidaceae* species. It is largely collected in Eastern Mediterranean countries and produced on an average 20 tons in Turkey every year (Hossain, 2011). The tubers of naturally grown orchids are dried and then ground to produce salep powder. Glucomannan is the most important polysaccharide constituent in salep. Salep is commonly used as a traditional beverage and a stabilizer for hard serve ice cream. As a hydrocolloid, the rheological behavior of salep in different food systems has been extensively reported in the literature (Ayar, Sert, & Akbulut, 2009; Karaman, Yilmaz, & Kayacier, 2013; Razavi & Karazhiyan, 2009; Tekinşen & Güner, 2010; Yasar, Kahyaoglu, & Sahan, 2009; Yilmaz, Karaman, & Kayacier, 2013). Hydrocolloids are also the main sources of edible films. In contrast, there is no report on the film-forming properties of salep glucomannan.

Edible films are defined as a thin layer placed on or between food components. Polysaccharides and proteins are used with plasticizers to form the film. Edible and biodegradable films can be used to reduce the migration of moisture, oxygen, and carbon dioxide, which improves the shelf-life and appearance of food products. The barrier, mechanical and thermal properties are the significant characteristics that are evaluated for the application of films. The utilization of renewable sources, such as hydrocolloids, for edible films is of primary interest for researchers due to its economic and environmental impact of them (Cerqueira et al., 2011).

Glucomannan and galactomannan has attracted considerable attention because of abundance, film forming capacity and biodegradability of them (Mikkonen and Tenkanen, 2012; Tester and Al-Ghazzewi, 2013). Among the glucomannan, the KGM edible

* Corresponding author at: Food Engineering Department, Chemistry & Metallurgical Faculty, Yildiz Technical University, Davutpasa Campus 34210, Istanbul, Turkey. Tel.: +90 212 383 4577; fax: +90 212 383 4571.
E-mail address: talipk@yildiz.edu.tr (T. Kahyaoglu).

0144-8617/$ – see front matter © 2014 Elsevier Ltd. All rights reserved.
http://dx.doi.org/10.1016/j.carbpol.2014.01.003

film has been widely studied (Mikkonen, 2009). However, SG has not been investigated from a film-forming perspective. Nieto (2009) reported that linear, high molecular weight, non-ionic polysaccharide gums form strong films. Pourjavadi et al. (2013) reported similar properties for salep glucomannan. Therefore, SG could be an alternative biodegradable film and an enhancer of film properties as KGM, which was used to obtain a highly functional blend film by mixing with different polymers, such as starch and gelatin (Chambi & Grosso, 2011; Chen, Liu, Chen, Chen, & Chang, 2008; Nair, Jyothi, Sajeev, & Misra, 2011).

There is no published information about the film-forming properties of salep glucomannan. Therefore the main objectives of this study were (i) to evaluate the edible film-forming properties of salep glucomannan (as a new source) for the first time; (ii) to compare its physical, mechanical, barrier, and thermal properties with locust bean and guar gum films.

2. Materials and methods

2.1. Materials

Dried and finely ground salep roots were purchased from a supplier in Kastamonu, Turkey. Guar gum and locust bean gum were kindly donated by Incom (Mersin, Turkey). The plasticizer glycerol (99% purity) was from Sigma Chemical Co. (St. Louis, MO, USA).

2.2. Film preparation

The plasticized glycerol films in this study were prepared by means of the casting and solvent evaporation method. In each solution, the weight of dry matter was 1.5 g per 100 mL water. Glycerol was added at 10% (w/w with respect to the amount of gum) in solution. Film-forming solutions were obtained by the solubilization of SG, GG, and LBG in 50 mL water by continual mixing in a water bath at 95 °C for 30 min. The film-forming solutions were centrifuged at 1500 g for 5 min to remove air bubbles and insoluble solids that could damage the film's appearance. The solutions (40 mL) were then cast in Teflon plates (13 cm diameter) and dried at 40 °C for 15 h to obtain dry films. Before the characterization of the physical, barrier, and mechanical properties, the films were kept in a conditioning desiccators at 43% (K_2CO_3 saturated solution) relative humidity (RH) for more than one week at room temperature to ensure the equilibrium of the water in the films. To determine the thermal sorption properties and FT-IR spectra, peeled films were conditioned under 0% RH (silica gels) at room temperature for a week before testing.

2.3. Rheological analysis of the film-forming solutions

The rheological measurements of the film-forming solutions were made with a rheometer (HAAKE Mars III; Thermo Scientific, Germany) with a cone and plate system (diameter: 3.5 mm, cone angle: 2°, gap between cone and plate: 0.105 mm). The samples were allowed to equilibrate for 5 min at the desired temperature (30, 60, 90 °C), and the measurements were then conducted at these temperatures. The shear rate increased linearly from 0 to 100 s^{-1} over 5 min. The flow behavior index (n) and consistency index (K) values were computed by fitting the power law model, Eq. (1).

$$\tau = K \times \gamma^n \quad (0 < n < 1) \tag{1}$$

where τ is the shear stress (Pa), γ is the shear rate (s^{-1}), K is the consistency index (Pa s^n), and n is the flow behavior index (dimensionless).

The consistency index, which is an indication of the viscous nature of the samples, was used to describe the variation in viscosity with temperature by fitting to the Arrhenius model, Eq. (2) (Farhoosh & Riazi, 2007).

$$\ln k = \ln A + \frac{E_A}{RT} \tag{2}$$

where A is the frequency factor (Pa s^n), E_A is the activation energy (kJ/mol), R is the universal gas constant (kJ/mol K), and T is the absolute temperature (K).

Oscillatory (dynamic) tests were conducted for all samples at 30, 60, 90 °C from 0.1 to 10 Hz at 1 Pa (in the linear viscoelastic range assessed by the stress sweep test). The samples were allowed to rest for 5 min after loading (gap between cone and plate: 0.7 mm). In these tests, the storage (G'), loss (G'') modulus (Pa), and tan δ (G''/G') were computed from raw data.

2.4. Physical properties of edible film

2.4.1. Moisture content

The moisture content of the films is stated as the percentage of water removed from the initial mass sample. It was analyzed gravimetrically by drying the samples at 105 °C for 24 h (AOAC, 2005). The experiments were performed on samples in triplicate.

2.4.2. Film thickness and density measurements

The thickness of the films was determined using a digital micrometer (Mitutoyo, Manufacturing Co. Ltd., Japan, 0.001 mm accuracy). Ten measurements were made at random positions on the film samples, and the mean values were calculated. The film density was determined from the ratio between the weight and volume (thickness × area). The density experiments were conducted in triplicate, and are reported as mean values.

2.4.3. Total soluble matter

The total soluble matter (TSM) of the films was calculated by employing the method described by Pelissari, Andrade-Mahecha, Sobral, and Menegalli (2013). The initial dry matter of the preconditioned film pieces (20 mm × 20 mm) was determined by drying in an air-circulating oven at 100 °C for 24 h (W_i). These film pieces were immersed in 50 mL distilled water containing sodium azide (0.002% w/v) to prevent microbial growth and stored at room temperature for 24 h under periodic agitation. The insoluble matter was separated carefully and dried at 105 °C for 24 h for determination of the final dry weight (W_f). All tests were carried out in triplicate, and the total soluble matter (%) in the film was calculated according to Eq. (3).

$$TSM = \frac{W_i - W_f}{W_i} \times 100 \tag{3}$$

where W_i is the initial dry matter of the sample (g) and W_f is the final dry matter of the sample (g).

2.5. Color and film transparency

The L (lightness), a (greenness and redness) and b (blueness and yellowness) values of the films were determined by a Minolta Chromameter (CR-400, Minolta Camera Co., Osaka, Japan). These values were determined by taking five readings at different positions on each film.

The film transparency was calculated according to the method of Park, Je, and Kim (2004) by measuring the film absorbance at 600 nm using a UV spectrophotometer (Helios Gama, England). The samples were cut into rectangular pieces based on the lateral area of the spectrophotometer test cell and placed in the test cell. The

reference value was determined from an empty test cell. The film transparency was calculated by Eq. (4).

$$T = \frac{Abs_{600}}{x} \quad (4)$$

where T is the transparency, Abs_{600} is the absorbance at 600 nm, and x is the mean film thickness (mm). According to this equation, high values of T indicate low transparency and a high degree of opacity. All the experiments were carried out in triplicate.

2.6. Water vapor permeability

The water vapor permeability (WVP) of the films was determined gravimetrically by following the standard test method (ASTM, 2003). Silica gel was used to obtain 0% RH in the interior of the glass cup. In order to remove possible water, glass cups containing silica gels were heated at 105 °C 24 h prior to use for sealing. Preconditioned film samples were sealed in cups with a 14 mm diameter with the aid of paraffin. The cups with covered film were stored in a desiccators containing distilled water (100% RH) at 25 °C. The weight of the cups was recorded at 0, 5, 15, 20, and 24 h. Determinations were made in triplicate, and WVP was calculated by Eq. (5).

$$WVP = \frac{w}{t} \times \frac{x}{\Delta P \times A} \quad (5)$$

where w/t is calculated by linear regression ($R^2 > 0.99$) from the water absorbed by the system at the steady state was reached. A is the film area exposed to moisture transfer (1.539×10^{-4} m^2), x is the mean sample thickness, and ΔP is the partial pressure difference through the film at 25 °C (kPa).

2.7. Oxygen barrier properties

A 25 mL conical flask was filled with 15 mL sunflower oil, covered with different films, sealed using paraffin and sticky tape, and stored at a controlled temperature (60 °C) for 10 days. The peroxide value of the sunflower oil samples was determined by sodium thiosulfate titration (AOCS, 1997). All the tests were carried out in triplicate.

2.8. Mechanical properties

Tensile strength (TS) and percentage of elongation at break (E%) were determined with a texture analyzer (Stable Micro System, Godalming, UK) based on the ASTM standard method 882 (ASTM, 2001). The films were cut in strips (1 cm × 10 cm) and conditioned for 3 days (43% RH). Before testing, the thickness of the strips was measured at ten points. The force and distance were recorded during the extension of the strips mounted between the grips at 2 mm/s until break. The results given are the average of five samples. The tensile strength and percentage elongation at the point at which the film broke was calculated with Eq. (6)–(7).

$$Tensile\ \ strength\,(TS) = \frac{\max imum\, force\,(N)}{thickness\,(m) \times width\,(m)} \quad (6)$$

$$E\% = 100 \times \frac{dr}{do} \quad (7)$$

where $E\%$ is the percentage of elongation at break, do is the distance onset of separation (cm), and dr is the distance of rupture (cm).

2.9. Water sorption isotherms

Sorption isotherms were measured according to the procedure described by Labuza (1984). The samples were cut into small pieces (15 mm × 20 mm) and dehydrated in a desiccators with silica gel (~0%) for 3 weeks. Before analysis, they were dried in a vacuum oven at 40 ± 2 °C (40 Torr). The dried samples were precisely weighed to the nearest 0.0001 g into small crucibles of aluminum foils, placed on tripods in jars and equilibrated in tightly closed jars containing different saturated salt solutions of known equilibrium relative humidities (RH/100, water activities) at 25 °C: NaOH = 0.08, KAc = 0.22, $MgCl_2$ = 0.32, K_2CO_3 = 0.43, $Mg(NO_3)_2$ = 0.52, KI = 0.68, NaCl = 0.75, KCl = 0.84, KNO_3 = 0.93. At high water activities ($a_w > 0.75$), a small amount of toluene was placed in a capillary tube fixed in the jar to prevent microbial spoilage of the samples. After the film samples reached equilibrium (15 days), the moisture content was determined by the oven-drying method at 105 °C for 24 h (AOAC, 2005). Isotherms were obtained by plotting the equilibrium moisture content of film samples versus the water activity (a_w). The Guggenheim, Anderson, and De Boer model (GAB) was used for data adjustment following Eq. (8).

$$X_W = \frac{c \times k \times m_o \times a_w}{[(1 - k \times a_w)(1 - k \times a_w + c \times k \times a_w)]} \quad (8)$$

where X_w is the equilibrium moisture content (g water/100 g dry solid), a_w is the water activity (RH/100), m_o is the monolayer moisture content (g water/100 g dry solid), C is the constant related to the monolayer heat sorption, and k is the constant related to the multilayer heat sorption. GAB model parameters were determined by non-linear regression using Statistica 10.0 software (StatSoft Inc., Oklahoma, USA).

2.10. Differential scanning calorimetry (DSC)

Thermal properties of the film samples (4–5 mg) were determined under nitrogen atmosphere with a Differential Scanning Calorimetry (DSC 4000, Perkin Elmer, USA) with a flow capacity of 20 mL/min from −55 to 300 at a heating rate 10 °C/min. The DSC was calibrated with indium (melting point = 156.6 °C, ΔH = 28.5 J/g). The glass transition temperature (T_g) was determined by taking the first derivative of the thermograms. T_g is the midpoint of the step, which indicates the glass transition in the baseline of DSC plot. All measurements were performed in duplicate, and the results are presented as mean values.

2.11. Fourier transform infrared spectroscopy (FT-IR)

The FT-IR spectra of films were recorded on a spectrophotometer (Perkin Elmer, Model Spectrum Two, Ohio, USA) fit with a Miracle Single-Reflection Diamond ATR device in the wavelength range of 4000–650 cm^{-1} with a spectral resolution of 4 cm^{-1}.

2.12. Statistical analysis

Microsoft Windows Excel® 2007 and SPSS software (Version 16.0, SPSS Inc., Chicago, USA) were used to analyze the data. The means were compared by Tukey's test at a 5% level of significance using analysis of variance (ANOVA).

3. Results and discussion

3.1. Rheological properties of the film solutions

Determining the rheological properties of film or coating solutions is critical for process scale up to ensure that processing requirements and machinability issues can be properly addressed (García, Pinotti, Martino, & Zaritzky, 2009). These properties also affect the presence or absence of defects in thin liquid films after coating (Nair et al., 2011; Wu, Zhong, Li, Shoemaker, & Xia, 2013).

Nonuniform films are the result of high or low viscosity, thus moderate viscosity is a positive character for film-forming solutions (Wu et al., 2013).

The apparent viscosity of all mannan samples decreased at all temperatures with increasing shear rate. This behavior is evidence of shear-thinning (pseudoplastic) properties ($n < 1$). The consistency index (K) and flow behavior index (n) values obtained from the power law model were used to compare the rheological characteristic of the samples ($R^2 = 0.968–0.999$) (Table 1). It is obvious that n values increased and K values decreased with increasing temperature. SG had higher n values than LBG and GG at all temperatures, indicating that LBG and GG were more pseudoplastic. In addition, the K values of galactomannans, especially GG, were higher than those of SG. The shear-thinning behavior of the salep solution has been reported by several authors (Dogan & Kayacier, 2004; Farhoosh & Riazi, 2007; Kaya & Tekin, 2001; Yaşar et al., 2009). Some authors have suggested a viscosity lower than 700 mPa s for coating applications (Nair et al., 2011). However, most edible film processes require uniform mixing, pumping solutions through filters and transfer lines to the film casting line and spreading the solution smoothly, for which an appropriate viscosity is 1000–10,000 mPa s (Rossman, 2009). In the present study, the SG film solution is appropriate for film casting and coating applications (239 mPa s). For processing, the appropriate range can be achieved by increasing the concentration.

The temperature of the film solution will also impact the viscosity, so determining the temperature dependency of the viscosity is important. As expected, a decrease in viscosity was observed with increasing temperature (Table 1). As the temperature increases, the thermal energy of the molecules and molecular distances increases due to acceleration of molecular movement so the viscosity of the fluid decreases (Farhoosh & Riazi, 2007). The temperature dependency of K was successfully assessed by applying the Arrhenius model ($R^2 = 0.929–0.971$). The activation energy (E_A) of the SG, LBG, and GG solutions was 13.777, 32.185, and 17.197 kJ/mol, respectively. In general, higher activation energy means a greater temperature effect on the viscosity (Koocheki, Mortazavi, Shahidi, Razavi, & Taherian, 2009). The lowest E_A was obtained for SG solutions, indicating that SG had the lowest viscosity dependency on the temperature. The outcomes imply that temperature control is more critical for galactomannans.

Dynamic rheological experiments can be used for the determination of the viscoelastic properties of samples. The elastic modulus (G') and loss modulus (G'') as a function of frequency (Hz) for film solutions at 30, 60, and 90 °C are shown in Fig. 1. These parameters at a frequency of 1 Hz are shown in Table 1. The G' and G'' of film solutions were dependent on frequency, indicating viscoelastic structure. A predominantly viscous behavior was observed for the SG and LBG film solutions up to nearly 1 Hz ($G'' > G'$) at all temperatures. In contrast, for GG solutions, the G' value was higher than G'' at low frequencies, so it exhibited gel-like behavior (Yaşar et al., 2009). The crossover frequency ($G' = G''$) of GG solutions occurred at 0.147, 0.147, and 0.464 Hz at 30, 60, and 90 °C, respectively, and then the elastic response prevailed ($G'' > G'$). An increased crossover frequency may be a consequence of decreasing relaxation time with temperature. Bourbon et al. (2010) reported viscous behavior ($G'' > G'$) for LBG solutions (1% gum concentration). The crossover frequency also reported above 1 Hz for GG solutions (0.98% gum concentration) at 25 °C. The significantly higher G'' compared to G' for LBG in our study may be due to the glycerol content of samples. GG film solution in this study (1.5% gum concentration) had lower crossover frequency since as the gum concentration increases, the crossover frequency decreases. tan δ values were also calculated to compare the viscoelastic properties of the film solutions. The film solution flows and spreads more easily at increased tan δ values. GG samples showed similar behavior at all temperatures ($p > 0.05$), but SG and LBG film solutions had a greater tan δ value than GG, and above 60 °C, a significant increase was observed for SG ($p < 0.05$). The comparison of the viscoelastic properties of film solutions at different temperatures and frequencies may yield better processing conditions.

3.2. Physical properties of films

3.2.1. Moisture content

The moisture content of the films is considered because of the plasticizer effect of water. Table 2 shows the moisture content of the films (conditioned at 43% RH). These different moisture content values ($p < 0.05$) of the films might be attributable to their different chemical structures and hygroscopicities. Due to its hydrophilic properties, the highest percentage of moisture content was found for the SG film (19.13%).

3.2.2. Film thickness and density measurements

The thickness value affects the permeability, mechanical properties and transparency of the film. The film made with SG had the lowest film thickness (0.025 mm). Similar thickness values were obtained for galactomannans films (0.034 and 0.033 mm for LBG and GG, respectively, $p > 0.05$; Table 2). The SG film presented significantly higher density than galactomannan films ($p < 0.05$; Table 2). This phenomenon may be due to the increased interaction between the molecular chains of the SG film. Pelissari et al. (2013) reported that the compositions, molecular weight and interaction components of the polymeric film structure are responsible for

Table 1
Apparent viscosity ($20\ s^{-1}$), power law parameters[a] and dynamic modulus[b] ($f = 1$ Hz) of film solutions[c] prepared with 10% glycerol at different temperatures.[d]

Temperature (°C)	Viscosity (Pa s)	K	n	R^2	G' (Pa)	G'' (Pa)	tan δ
SG							
30	0.296 ± 0.001[b]	0.716 ± 0.005[a]	0.716 ± 0.006[f]	0.999	0.602 ± 0.008[ab]	1.926 ± 0.226[b]	3.198 ± 0.007[d]
60	0.177 ± 0.001[ab]	0.653 ± 0.005[a]	0.670 ± 0.001[f]	0.993	0.384 ± 0.039[ab]	1.172 ± 0.062[ab]	3.063 ± 0.152[d]
90	0.056 ± 0.001[a]	0.113 ± 0.005[a]	0.730 ± 0.007[f]	0.984	0.041 ± 0.007[a]	0.438 ± 0.008[a]	11.89 ± 0.155[e]
LBG							
30	2.509 ± 0.084[f]	12.09 ± 0374[c]	0.474 ± 0.001[d]	0.993	10.350 ± 0.197[e]	16.475 ± 0.332[f]	1.581 ± 0.016[b]
60	1.481 ± 0.067[d]	5.508 ± 0.332[b]	0.570 ± 0.035[e]	0.968	5.351 ± 0.215[c]	9.331 ± 0.064[e]	1.745 ± 0.057[b]
90	0.588 ± 0,011[c]	1.431 ± 0.130[a]	0.707 ± 0.022[f]	0.996	1.847 ± 0.513[b]	3.980 ± 0.759[c]	2.182 ± 0.195[c]
GG							
30	3.668 ± 0.074[h]	40.150 ± 1.414[e]	0.191 ± 0.007[a]	0.998	30.840 ± 0.537[g]	17.545 ± 0.445[f]	0.568 ± 0.004[a]
60	2.766 ± 0.060[g]	23.705 ± 0.855[d]	0.280 ± 0.014[b]	0.996	28.200 ± 0.777[f]	17.570 ± 0.989[f]	0.611 ± 0.002[a]
90	1.799 ± 0.102[e]	12.925 ± 0.657[c]	0.341 ± 0.002[c]	0.993	8.809 ± 0.030[d]	7.834 ± 0.014[d]	0.889 ± 0.001[a]

[a] K: consistency index; n: flow behavior index; R^2: coefficients of determinations.
[b] G': elastic modulus; G'': loss modulus; tan δ: G''/G'.
[c] SG: salep glucomannan; LBG: locust bean gum; GG: guar gum.
[d] Different letters in the same column indicate statistically significant differences ($p < 0.05$). Values are the means of three measurements of two replicates (mean ± standard deviation).

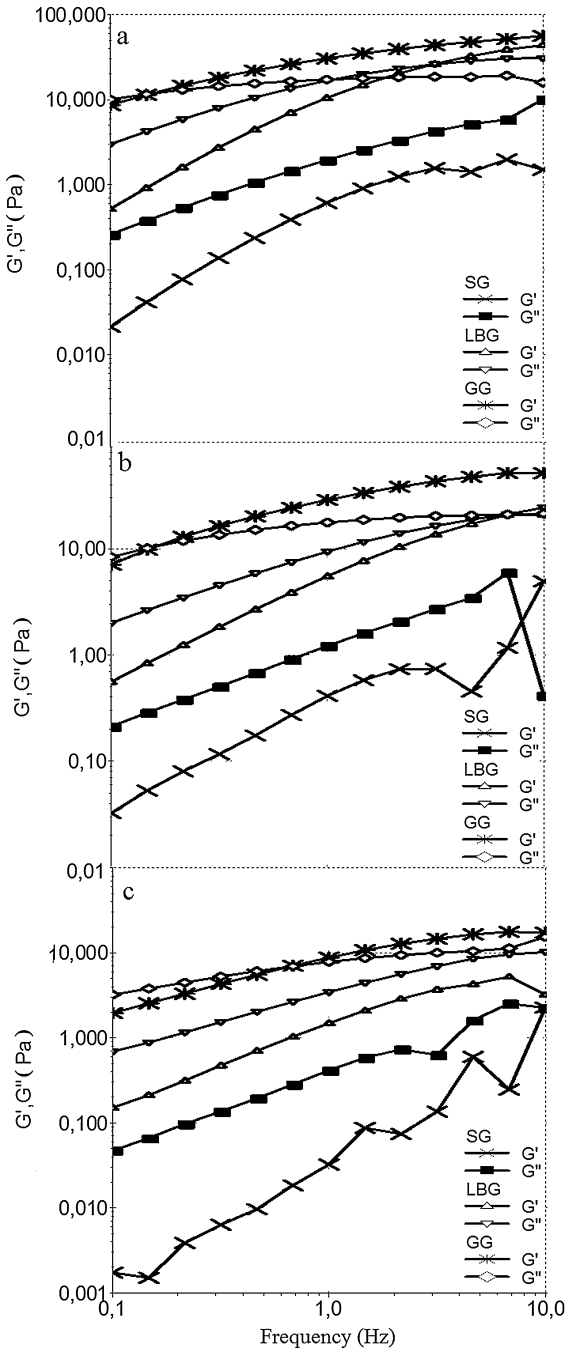

Fig. 1. Elastic modulus (G') and loss modulus (G'') of film solutions at 30 °C (a), 60 °C (b), and 90 °C (c) (SG: salep glucomannan; LBG: locust bean gum; GG: guar gum).

different density values. This result is consistent with the mechanical properties, water vapor and oxygen permeability values of the SG film obtained in this study. Compared with other biodegradable films, the density values obtained for the SG film (1.27 g/cm^3) are lower than those found for cassava starch films (1.38 g/cm^3) (Famá, Gerschensen, & Goayanes, 2009) and whey protein isolate films plasticized at different glycerol concentrations (40, 50, and 60%), similar to whey protein concentrate film (Ramos et al., 2013) and higher than keratin films (0.92–1.10 g/cm^3) plasticized with different glycerol concentrations (Moore, Martelli, Gandolfo, Sobral, & Laurindo, 2006).

3.2.3. Solubility in water

Film solubility is an important property for edible films. The desired solubility value depends on the application or intended use. The solubility of the SG film in water is higher than that of galactomannan films ($p < 0.05$; Table 2). Because of the high moisture content of SG, crosslinking between biopolymer molecules is most likely reduced in swollen film structure (Ahmadi, Kalbasi-Ashtari, Oromiehie, Yarmand, & Jahandideh, 2012). In the present study, the SG film has the highest moisture content and solubility values, indicating low water resistance. Water solubility values between 17.33 and 19.89% for potato starch film (Zavareze et al., 2012), 38.8% for cassava starch film (Nair et al., 2011), and 40–50% for KGM film (Li, Peng, Yie, & Xie, 2006) have been reported.

3.2.4. Optical properties

Film color and transparency are important parameters for general appearance and consumer acceptance. The L, a, and b values of the films are shown in Table 2. There were no significant differences in the L values of all samples ($p > 0.05$). High a values show that these films tend to be reddish. The a value of the SG film was not significantly different from that of the galactomannan films ($p > 0.05$). The LBG film presented as less yellowish (b value) compared to the other films ($p < 0.05$). Martins et al. (2012) reported color values for LBG film of $L = 97.54$, $a = 5.26$, and $b = -3.29$. These a and b color parameter values are higher and the L value lower than the values reported in the present study. The transparency of the films is summarized in Table 2. Transparency values for the films were significantly different ($p < 0.05$). SG film was the most transparent as indicated by the low T value. Galactomannan films with high opacity were characterized by high transparency. In this study, the T value of the SG film was similar to that of low-density polyethylene films (LDPE) (3.05) and higher than oriented polypropylene (OPP) and polyethylene (PE), which were 1.67 and 1.51, respectively (Ramos et al., 2013).

3.3. Water vapor permeability

The water vapor permeability (WVP) of films should be as low as possible to reduce moisture transfer between the food and surrounding atmosphere. This property is related to the film structure, plasticizer, RH gradient and temperature of the environment. The WVP of the edible films is shown in Table 3. The WVP exhibited the following trend: SG < LBG < GG. Although the SG film had the lowest WVP among the samples, there were no significant differences between the WVP of SG and LBG films used in the present work ($p > 0.05$). This result may be explained by lower molecular mobility of SG and LBG than GG film. Because SG doesn't contain galactose branches and LBG is lower substituted with galactose than

Table 2
Physical properties (moisture content, thickness, density, solubility, color (L, a, b), and transparency (T)) of film samples[a,b].

Sample code	Moisture content (d.b.%)	Thickness (mm)	Density (g cm^{-3})	Solubility (%)	L	a	b	T
SG	19.13 ± 0.02^{c}	0.025 ± 0.000^{a}	1.27 ± 0.02^{b}	92.98 ± 0.67^{c}	81.61 ± 0.11^{a}	5.79 ± 0.06^{ab}	1.28 ± 0.21^{b}	3.74 ± 0.08^{a}
LBG	8.54 ± 0.03^{a}	0.034 ± 0.001^{b}	1.12 ± 0.03^{a}	57.87 ± 0.74^{a}	81.75 ± 0.26^{a}	5.91 ± 0.00^{b}	0.67 ± 0.05^{a}	5.22 ± 0.01^{c}
GG	11.31 ± 0.02^{b}	0.033 ± 0.000^{b}	1.14 ± 0.01^{a}	75.94 ± 0.38^{b}	81.82 ± 0.15^{a}	5.69 ± 0.03^{a}	1.28 ± 0.18^{b}	4.30 ± 0.08^{b}

[a] SG: salep glucomannan; LBG: locust bean gum; GG: guar gum.
[b] Different letters in the same column indicate statistically significant differences ($p < 0.05$). Values are the means of three measurements of two replicates (mean ± standard deviation).

Table 3
Water vapor permeability (WVP) and peroxide value (PV) of the oil samples protected by film samples and the elongation at break (EB) and tensile strength (TS) of the films[a,b].

Sample code	WVP ($g\,mm\,h^{-1}\,m^{-2}\,kPa^{-1}$)	PV (meq/kg)	EB (%)	TS (MPa)
SG	0.097 ± 0.001^{a}	91.20 ± 1.06^{a}	37.2 ± 0.15^{c}	49.59 ± 3.53^{a}
LBG	0.122 ± 0.004^{a}	94.19 ± 1.01^{ab}	26.0 ± 2.07^{b}	71.41 ± 4.41^{b}
GG	0.164 ± 0.001^{b}	95.04 ± 0.13^{b}	16.1 ± 0.59^{a}	42.84 ± 1.22^{a}

[a] SG: salep glucomannan; LBG: locust bean gum; GG: guar gum.
[b] Different letters in the same column indicate statistically significant differences ($p < 0.05$). Values are the means of three measurements of two replicates (mean ± standard deviation).

GG (Mikkonen, 2009; Pourjavadi et al., 2013). Mikkonen, Heikkilä, Helén, Hyvönen, and Tenkanen (2010) studied the WVP of mannan films. They found that the WVP of KGM films at a 0/54% RH gradient was higher than that of LBG and GG films. GG film had also higher WVP values than LBG film, similar to the results of the present study.

The WVP value of SG film obtained in this study ($0.097\,g\,mm\,h^{-1}\,m^{-2}\,kPa^{-1}$) was also lower than that reported by Chambi (2011) for KGM, pectin, and methylcellulose films, which were 0.204, 0.282, and $0.294\,g\,mm\,h^{-1}\,m^{-2}\,kPa^{-1}$, respectively. The WVP values of LBG film obtained in the present study are lower than those previously reported for glycerol-plasticized (30%) LBG films by Martins et al. (2012). They found the WVP of LBG films to be $8.01 \times 10^{-11}\,g\,(m\,s\,Pa)^{-1}$, which corresponds to $0.288\,g\,mm\,h^{-1}\,m^{-2}\,kPa^{-1}$. This result could be explained by the different glycerol levels of the films. Increasing glycerol may enhance water clustering on the polymer and increase the free volume of the film matrix, which promotes higher diffusivity and increased permeability (Ahmadi et al., 2012; Ramos et al., 2013).

3.4. Oxygen barrier properties

Oxygen permeability (OP) is another important barrier property because the oxidation of lipids and food ingredients causes a great deal of food deterioration (Janjarasskul & Krochta, 2010). To determine the oxygen barrier properties of films, a sunflower oil-filled conical flask was covered with the films (SG, LBG, and GG films) to prevent the oxidation of oil, and the peroxide value (PV) was calculated. The PV of mannan films displayed the following trend: GG > LBG > SG, which was the same order as the WVP (Table 3). The PV of the oil covered with the films ranged from 91.20 to 95.04 meq/kg, and for uncovered oil it was 110 ± 1.02 meq/kg. The results showed that all films reduced the oxidation of the oil, and the SG film had higher preventative ability than the LBG and GG films. These results may be explained by the denser packing of mannan chains in the SG film, which is possible because glucomannan does not contain galactose branches and the acetyl groups presented on mannan chains are smaller than those on galactose. Similar results were reported for the OP of KGM, which is lower than that of the GG and LBG films. The GG film had the highest level of OP (Mikkonen, 2009).

The SG film has a smooth surface, while an uneven and rough surface of GG and LBG films was visually observed. Film thickness also affects the oxygen permeability of films (Wu et al., 2013). The thinner film of this study provided by SG may show better performance at higher film thickness (Table 2).

3.5. Mechanical properties

The determination of the mechanical properties of polymer materials such as films involves not only scientific but also technological and practical aspects because the films may be subjected to various types of stress during use (Li et al., 2006; Lu, Wang, & Wang, 2008; Xiao, Lu, Gao, & Zhang, 2000). Tensile strength (TS) is obtained at the sample break point, and elongation at break (E%) is the increase in the sample length from its original length to the break point. TS and *E%* are used to determine the mechanical properties of the films and related them to the chemical structure (Zavareze et al., 2012). These parameters are indicators of the film strength and flexibility.

The mechanical properties of the films are presented in Table 3. The tensile strength (TS) followed the trend LBG > SG > GG. Statistical analysis indicated that there were no significant differences between the SG and GG films ($p > 0.05$). The TS value of SG (49.59 MPa) was different from that of the KGM film reported in literature. The TS for KGM films plasticized with 40% glycerol was reported to be 43 MPa by Mikkonen (2009) and (40).09 ± 1.89 MPa for 37.5% plasticized KGM films by Wu et al. (2012). The higher TS values of SG in this study may be due to the lower glycerol level (10%) of the film solutions because the plasticizer decreases the intermolecular forces along polymer chains, thus decreasing the rigidity of the network but increasing film flexibility. Glucomannan are often acetylated on mannosyl residues (Scheller & Ulskov, 2010; Teleman, 2009). The different acetyl groups of glucomannan may also affect the TS values of the films. The higher tensile strength of SG than KGM film could be due to the denser packing of mannan chains, resulting in increased hydrogen bonding because of the lower acetyl group in the SG.

The *E%* of SG films was higher, and these films showed more flexibility than galactomannans films ($p < 0.05$). The *E%* of polymeric materials depends on the flexibility of the molecular chain (Zavareze et al., 2012). These results may also correspond to the higher moisture content of SG films because of the plasticizing effects of water (Table 2).

Comparing the TS values for SG obtained in this study to those reported for synthetic films, the SG films exhibited higher values than low-density polyethylene (LDP) (23–28 MPa) and lower values than cellophane (114 MPa). In contrast, the EB values of SG were lower than LDP films (100%) but higher than cellophane (20%) (Chambi, 2011).

3.6. Water sorption isotherms

The water adsorption of hydrophilic films is important for film stability and applications depending on the environmental relative humidity. Fig. 2 shows the water sorption isotherm of mannan films together with the GAB model fitted for each film. The parameters of the GAB model and coefficient determinations are given in Table 4. The coefficient of determination ($R^2 > 0.99$) shows that the GAB model can be used to fit the experimental data. In general, the moisture adsorption isotherms display a sigmoid shape, which is typical of films. All mannan films obtained in this study showed similar patterns. The equilibrium moisture contents of films increased slowly until a_w 0.6; thereafter, a sharp increase occurred. That type of nonlinear sorption profile is the usual result for hydrophilic films (Kibar & Us, 2013). SG and LBG film showed a higher adsorption capacity than GG film (Fig. 2). The monolayer moisture content (m_0) of the film indicates the

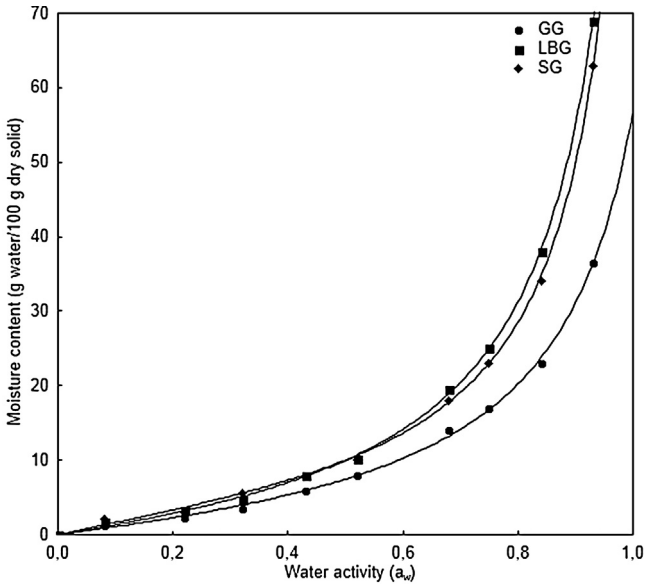

Fig. 2. Water sorption isotherms of films fit with the GAB model. Symbols are the experimental data, and lines are the GAB-fitted curves (SG: salep glucomannan; LBG: locust bean gum; GG: guar gum).

Table 4
GAB model parameters for the water sorption isotherms of the film samples[a,b].

Sample code	m_0 (g water/100 g dry solid)	k	C	R^2
SG	7.77 ± 0.33	0.95 ± 0.00	2.12 ± 0.30	>0.99
LBG	9.64 ± 0.53	0.93 ± 0.01	1.37 ± 0.19	>0.99
GG	7.85 ± 0.94	0.87 ± 0.01	1.47 ± 0.34	>0.99

[a] SG: salep glucomannan; LBG: locust bean gum; GG: guar gum.
[b] m_0: monolayer value; C: Guggenheim constant related to the monolayer heat sorption, k: constant related to the multilayer heat sorption, R^2: coefficient of determination.

number of active sites available for strong adsorption of water at the surface. Therefore, it could be concluded that SG film has a low number of available sorption sites (Table 4). Because of its acetyl groups, SG has a more hydrophobic character than galactomannans, which have a free hydroxyl groups in their sugar units (Mikkonen, 2009). The constants in the GAB equation (k and C) are temperature-dependent parameters. The k values obtained for the films were <1. The C parameter, which is related to the monolayer heat sorption, was higher for SG film than for galactomannan films.

3.7. DSC analysis

The thermal behavior of the films was investigated by DSC measurements (Fig. 3). The endothermic peaks of films approximately 50–150 °C was attributed to the loss of a small amount of moisture. SG films revealed decomposition peaks at 255 °C and showed similar thermo-stability with galactomannan films (Fig. 3a). Although preparation, plasticizer and storage conditions impact the thermal properties of film, it should be noted that the SG films obtained in the present study also had higher thermostability than that of KGM, which was previously reported as 228.4 °C (Lu et al., 2008) and 220.9 °C (Wu et al., 2012). The first derivation of the thermograms indicates whether there is a glass transition in the base line or not (Kibar et al., 2013). The films exhibit only one glass transition temperature (T_g), indicating a homogeneous mixture of the compounds, especially glycerol, in the film matrix (Pelissari et al., 2013). The T_g of the films was detected as -11.46 ± 0.65, -12.14 ± 0.08, and -15.43 ± 0.60 °C for SG, LBG, and GG, respectively (Fig. 3b). There were no significant differences between the SG and LBG films ($p > 0.05$). The lower T_g value of the GG film indicates higher free volume, resulting in higher molecular mobility of the polymer film matrix due to the hindrance effect of galactose between polymer chains. It was shown that the mannan films presented in this study are in a rubbery state at room temperature (T_g <0 °C). These results are also supported by the work of Mikkonen (2009), who reported that the T_g of KGM, GG, and LBG films was below 0 °C.

3.8. FT-IR analysis

IR spectra were used to characterize the structure of the polysaccharides. The FT-IR spectra of mannan films from 4000 to 650 cm^{-1} are shown in Fig. 4. A broad peak located approximately 3303 cm^{-1} was assigned to the stretching vibration of O—H groups, which was affected by inter-molecular and intra-molecular hydrogen bonds. C—H aliphatic absorption peaks are located at 2937, 2923, and 2926 cm^{-1} for GG, LBG, and SG, respectively. The small peak for SG film at 1731 cm^{-1} is due to the C=O stretching vibration (Chua et al., 2012). The broad peak approximately 1640 cm^{-1} in the spectrum of mannan films is attributed to the existence of water. Wu et al. (2012) reported same peak at 1647 cm^{-1} for native konjac glucomannan. The peaks approximately 1150, 1052, and 1033 cm^{-1} usually correspond to C—O—C asymmetric and symmetric

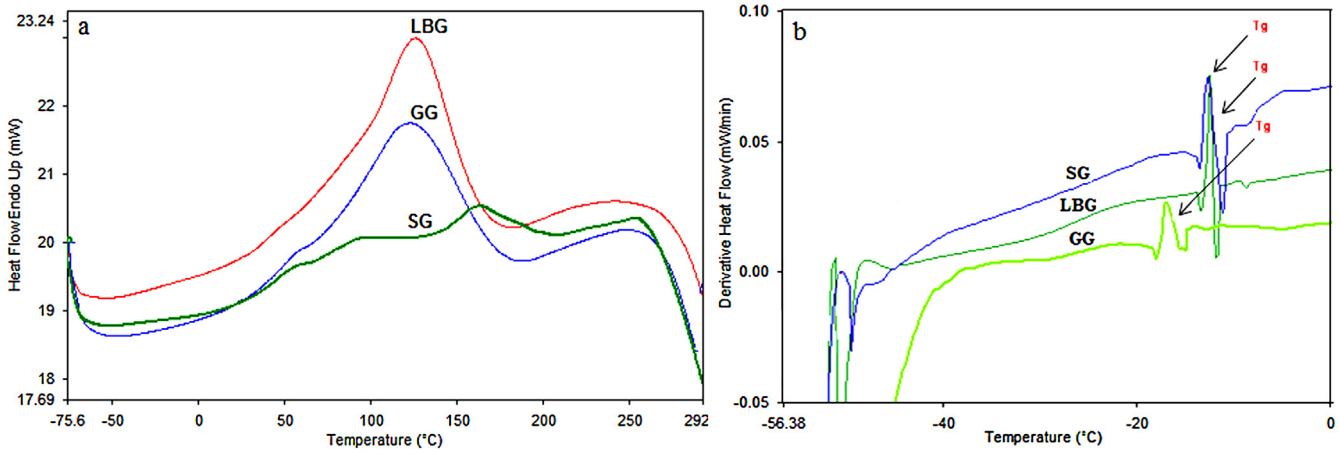

Fig. 3. DSC thermograms of films (SG: salep glucomannan; LBG: locust bean gum; GG: guar gum). (a) The first derivatives of heat flow curves. (b) The glass transition temperatures (T_g) were marked on the first derivatives of the heat flow curves.

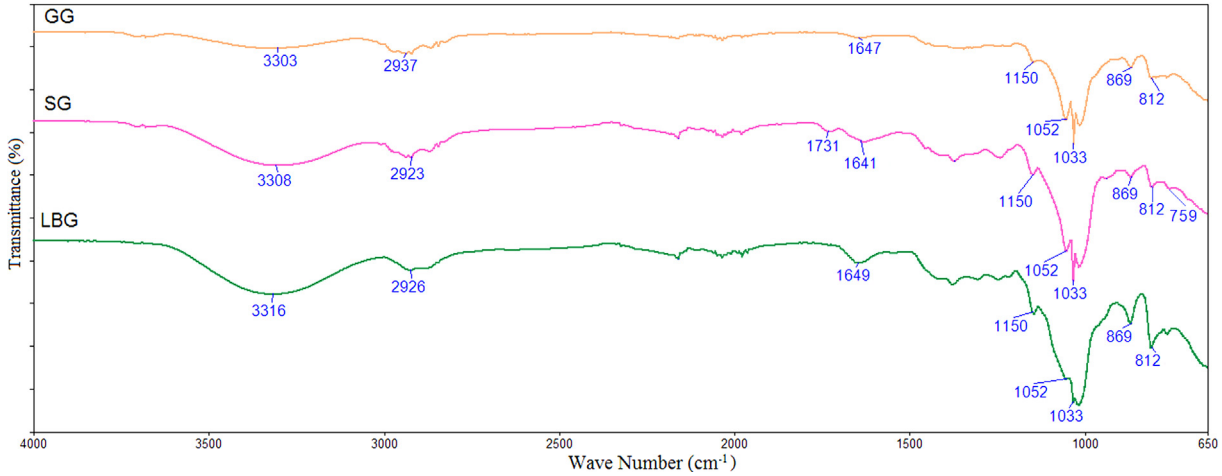

Fig. 4. FT-IR spectra of films (SG: salep glucomannan; LBG: locust bean gum; GG: guar gum).

stretching modes from ether group in the pyranose rings (Chua et al., 2012; Pourjavadi et al., 2013). The characteristic peaks observed at ~869 and ~812 cm^{-1} are attributed to β-glucosidic and β-mannosidic linkages, respectively, for all films. The existence of an absorption peak at 759 cm^{-1} indicated the aromatic structures of SG films (Pelissari et al., 2013). Based on the results of FT-IR, the SG film showed structural properties similar to the galactomannan films.

4. Conclusion

This is the first report that salep glucomannan has good film-forming properties and potential application as an edible food film and coating. SG film solutions showed similar viscoelastic properties compared to LBG. SG films showed better oxygen and water vapor barrier properties than LBG and GG films. The mechanical characteristics of SG films were comparable with galactomannans and had better properties than GG films. The structural properties of SG and galactomannan films were similar based on the FT-IR spectra. SG films could be manipulated to some extent by adjusting the concentration of the film solution. Other studies should be conducted to reduce the solubility of SG (92.98%) and thereby improve the properties of the SG film. Because of potential compatibility with other polysaccharides that may yield synergistic effects, salep glucomannan may also be of use in improving functionality by tailoring film properties.

References

Ahmadi, R., Kalbasi-Ashtari, A., Oromiehie, A., Yarmand, M., & Jahandideh, F. (2012). Development and characterization of a novel biodegradable edible film obtained from psyllium seed (*Plantago ovata* Forsk). *Journal of Food Engineering*, *109*, 745–751.

AOAC. (2005). *Official methods of analysis (18th ed.)*. Washington: Associations of Official Analytical Chemists.

AOCS. (1997). *Official methods and recommended practices of analysis of association of official chemist*. AOCS, 5th edition, 2nd Printing.

ASTM. (2001). Standard Test Method for Tensile Properties of Thin Plastic Sheeting. In *Standard designations D 882*. Philadelphia: American Society for Testing and Materials.

ASTM. (2003). *Annual book of ASTM standards*. Pennsylvania: American Society for Testing and Materials.

Ayar, A., Sert, D., & Akbulut, M. (2009). Effect of salep as a hydrocolloid on storage stability of İncir Uyutması dessert. *Food Hydrocolloids*, *23*, 62–71.

Bourbon, A. I., Pinheiro, A. C., Ribeiro, C., Miranda, C., Maia, J. M., Teixeira, J. A., & Vicente, A. A. (2010). Characterization of galactomannans extracted from seeds of *Gleditsia triacanthos* and *Sophora japonica* through shear and extensional rheology: Comparison with guar gum and locust bean gum. *Food Hydrocolloids*, *24*, 184–192.

Cerqueira, M. A., Bourbon, A. I., Pinheiro, A. C., Martins, J. T., Souza, B. W. S., Teixeira, J. A., & Vicente, A. A. (2011). Galactomannans use in the development of edible films/coatings for food applications. *Trend in Food Science & Technology*, *22*, 662–671.

Chambi, H. N. M., & Grosso, C. R. F. (2011). Mechanical and water vapor permeability properties of biodegradables films based on methylcellulose, glucomannan, pectin and gelatin. *Ciência Tecnologia Alimentos Campinas*, *31*(3), 739–746.

Chen, J., Liu, C., Chen, Y., Chen, Y., & Chang, P. R. (2008). Structural characterization and properties of starch/konjac glucomannan blend films. *Carbohydrate Polymers*, *74*, 946–952.

Chua, M., Chan, K., Trevor, J. H., Williams, P. A., Christopher, J. P., & Baldwin, T. C. (2012). Methodologies for the extraction and analysis of konjac glucomannan from corms of *Amorphophallus konjac* K. Koch. *Carbohydrate Polymers*, *87*, 2202–2210.

Dogan, M., & Kayacier, A. (2004). Rheological properties of reconstituted hot salep beverage. *International Journal of Food Properties*, *7*(3), 683–691.

Famá, L., Gerchenson, L., & Goyanes, S. (2009). Starch-vegetable fibre composites to protect food product. *Carbohydrate Polymers*, *75*(2), 230–235.

Farhoosh, R., & Riazi, A. (2007). A compositional study on two current types of salep in Iran and their rheological properties as a function of concentration and temperature. *Food Hydrocolloids*, *21*, 660–666.

García, M. A., Pinotti, A., Martino, M. N., & Zaritzky, N. E. (2009). Characterization of starch and composite edible films and coatings. In M. E. Embuscado, & K. C. Huber (Eds.), *Edible films and coatings for food applications* (pp. 169–209). London/New York: Springer Dordrecht Heildelberg.

Hossain, M. M. (2011). Therapeutic orchids: Traditional uses and recent advances—an overview. *Fitoterapia*, *82*, 102–140.

Janjarasskul, T., & Krochta, J. M. (2010). Edible packaging materials. *Annual Review of Food Science and Technology*, *1*, 415–448.

Karaman, S., Yilmaz, M. T., & Kayacier, A. (2013). Mathematical approach for two component modeling of salep-starch mixtures using central composite rotatable design: Part II. Dynamic oscillatory shear properties and applicability of Cox–Merz rule. *Food Hydrocolloids*, *31*, 277–288.

Kaya, S., & Tekin, A. R. (2001). The effect of salep on the rheological characteristic of a typical ice-cream mix. *Journal of Food Engineering*, *47*, 59–62.

Kibar, E. A. A., & Us, F. (2013). Thermal mechanical and water adsorption properties of corn starch-carboxymethylcelluso/methylcelluso biodegradable films. *Journal of Food Engineering*, *114*, 123–131.

Koocheki, A., Mortazavi, S. A., Shahidi, F., Razavi, S. M. A., & Taherian, A. R. (2009). Rheolgical properties of mucilage extracted from *Alyssum homolocarpum* seed as a new source of thickening agent. *Journal of Food Engineering*, *91*, 490–496.

Labuza, T. P. (1984). *Practical aspects of isotherm measurement and use*. St. Paul Minnesota: American Association of Cereal Chemists.

Li, B., Peng, J., Yie, X., & Xie, B. (2006). Enhancing physical properties and antimicrobial activity of konjac glucomannan edible films by incorporating chitosan and nisin. *Journal of Food Science*, *71*(3), 174–178.

Lu, J., Wang, X., & Xiao, C. (2008). Preparation and characterization of konjac glucomannan/poly(diallydimethylammonium chloride) antibacterial blend films. *Carbohydrate Polymers*, *73*, 427–437.

Martins, J. T., Cerqueira, M. A., Bourbon, A. I., Pinheiro, A. C., Souza, B. W. S., & Vicente, A. A. (2012). Synergistic effects between (-carrageenan and locust bean gum on physicochemical properties of edible films made thereof. *Food Hydrocolloids*, *29*, 280–289.

Mikkonen, K. S. (2009). *Mannans as film formers and emulsion stabilizers*. Finland: Department of Applied Chemistry and Microbiology Department of Food Technology University of Helsinki.

Mikkonen, K. S., Heikkilä, M. I., Helén, H., Hyvönen, L., & Tenkanen, M. (2010). Spruce galactoglucomannan films show promising barrier properties. *Carbohydrate Polymers*, *79*, 1107–1112.

Mikkonen, K. S., & Tenkanen, M. (2012). Sustainable food-packaging materials based on future biorefinery products: Xylans and mannans. *Trends in Food Science & Technology*, *28*, 90–102.

Moore, G. R. P., Martelli, S. M., Gandolfo, C., Sobral, P. J. A., & Laurindo, J. B. (2006). Influence of the glycerol concentration on some physical properties of feather keratin films. *Food Hydrocolloids*, *20*, 975–982.

Nair, S. B., Jyothi, A. N., Sajeev, M. S., & Misra, R. (2011). Rheological, mechanical and moisture sorption characteristics of cassava starch-konjac glucomannan blend films. *Starch-Starke*, *63*, 728–739.

Nieto, M. B. (2009). Structure and function of polysaccharide gum-based edible films and coatings. In M. E. Embuscado, & K. C. Huber (Eds.), *Edible films and coatings for food applications* (pp. 57–112). London New York: Springer Dordrecht Heildelberg.

Park, P., Je, J., & Kim, S. (2004). Free radical scavenging activities of differently deacetylated chitosans using an ESR spectrometer. *Carbohydrate Polymers*, *55*, 17–22.

Pelissari, M. C., Andrade-Mahecha, M. M., Sobral, P. J. A., & Menegalli, F. C. (2013). Comparative study on the properties of flour and starch of plantain bananas (*Musa paradisiaca*). *Food Hydrocolloids*, *30*, 681–690.

Pourjavadi, A., Fakoorpoor, S. M., & Hosseine, S. H. (2013). Novel cationic-modified salep as an efficient flocculation agent for settling of cement slurries. *Carbohydrate Polymers*, *93*, 506–511.

Ramos, Ó. L., Reinas, I., Silva, S. I., Fernandes, J. C., Cerqueira, M. A., Pereira, R. N., Vicente, A. A., Poças, M. F., Pintado, M. E., & Malcata, F. X. (2013). Effect of whey protein purity and glycerol content upon physical properties of edible films manufactured therefrom. *Food Hydrocolloids*, *30*, 110–122.

Razavi, S. M. A., & Karazhiyan, H. (2009). Flow properties and thixotropy of selected hydrocolloids: Experimental and modeling studies. *Food Hydrocolloids*, *23*, 908–912.

Rossman, J. M. (2009). Commercial manufacturate of edible films. In M. E. Embuscado, & K. C. Huber (Eds.), *Edible films and coatings for food applications* (pp. 367–390). London, New York: Springer Dordrecht Heildelberg.

Rowell, R. M., Pettersen, R., Han, J. S., Rowell, J., & Tshabalala, M. A. (2005). *Handbook of wood chemistry and wood composites*. CRC Press. Chapter 3.

Scheller, H. V., & Ulskov, P. (2010). Hemicelluloses. *Annual Review of Plant Biology*, *61*(1), 263–289.

Tekinşen, K. K., & Güner, A. (2010). Chemical compositon and physicochemical properties of tubera salep produced from some *Orchidaceae* species. *Food Chemistry*, *121*, 468–471.

Teleman, A. (2009). Hemicelluloses and pectins. In M. Ek, G. Gellerstedt, & G. Henriksson (Eds.), *Wood Chemistry and Biotechnology* (pp. 101–120). 10785 Berlin: Walter de Gruyter GmbH & Co. KG.

Tester, R. F., & Al-Ghazzewi, F. H. (2013). Mannans and health, with a special focus on glucomannans. *Food Research International*, *50*, 384–391.

Wu, C., Peng, S., Wen, C., Wang, X., Fan, L., Deng, R., & Pang, J. (2012). Structural characterization and properties of konjac glucomannan/curdlan blend films. *Carbohydrate Polymers*, *89*, 497–503.

Wu, J., Zhong, F., Li, Y., Shoemaker, C. F., & Xia, W. (2013). Preparation and charazterization of pullulan-chitosan and pullulan-carboxymethyl chitosan blended films. *Food Hydrocolloids*, *30*, 82–91.

Xiao, C., Lu, Y., Gao, S., & Zhang, L. (2000). Characterization of konjac glucomannan-gelatin blend films. *Journal of Applied Polymer Science*, *79*, 1596–1602.

Yasar, K., Kahyaoglu, T., & Sahan, N. (2009). Dynamic rheological characterization of salep glucomannan/galactomannan-based milk beverages. *Food Hydrocolloids*, *23*, 1305–1311.

Yilmaz, M. T., Karaman, S., & Kayacier, A. (2013). Mathematical approach for two component modeling of salep-starch mixtures using central composite rotatable design: Part I. Physicochemical and steady shear properties. *Food Hydrocolloids*, *31*, 49–60.

Zavareze, E. R., Pinto, V. Z., Klein, B., Halal, S. L. M. E., Elias, M. C., Hernández, P. C., & Dias, A. R. G. (2012). Development of oxidised and heat–moisture treated potato starch film. *Food Chemistry*, *132*, 344–350.